Journal of
Electrical & Electronic Systems

Elazzaoui, J Electr Electron Syst 2015, 4:1
DOI: 10.4172/2332-0796.1000141

Research Article Open Access

Modeling and Control of a Wind System Based Doubly Fed Induction Generator: Optimization of the Power Produced

Marouan Elazzaoui*

Department of Electrical Engineering, Electronic Power and Control Laboratory, Mohammedia School of Engineering Université Mohammed V-Agdal, Morocco

Abstract

This paper deals with the modeling and control of a wind energy system based on a doubly-fed induction generator. Initially, an MPPT control strategy of the doubly-fed induction generator is presented. Thereafter, the control vector-oriented stator flux is performed. Finally, the simulation results of the wind system using a doubly-fed of 3 MW are presented in the Matlab / Simulink environment.

Keywords: Wind turbine; Doubly-fed induction generator; Converter; Vector control

Introduction

Today, wind energy has become a viable solution for energy production, in addition to other renewable energy sources. While the majority of wind turbines are fixed speed, the number of variable speed wind turbines is increasing [1]. The doubly-fed induction generator with vector control is a machine that has excellent performance and is commonly used in the wind turbine industry [2]. There are many reasons for using a doubly-fed induction generator for a variable speed wind turbine; such as reducing efforts on the mechanical parts, reducing noise and the possibility of control of active and reactive power [3]. The wind system using DFIG and a "back-to-back" converter that connects the rotor of the generator and the network has many advantages (Figure 1).

One advantage of this structure is that the power converters used are dimensioned to pass a fraction of the total power of the system [4,5]. Thereby reducing losses in power electronic components. The performance and power production does not only depend on the DFIG, but also the way in which the two parts of "back-to-back" converter is controlled. The power converter machine side is called «Rotor Side Converter» (RSC) and the grid side power converter is called «Grid Side Converter» (GSC). The machine side power converter controls the active power and reactive power produced by the machine. As for the grid-side converter, it controls the DC bus voltage and line-side power factor. In this paper, we present a technique for controlling the two power converters. We will analyze their dynamic performance by simulations in Matlab / Simulink environment. We start with a model of the wind turbine,then a technique for continued operation at maximum power point tracking (MPPT) will be presented.

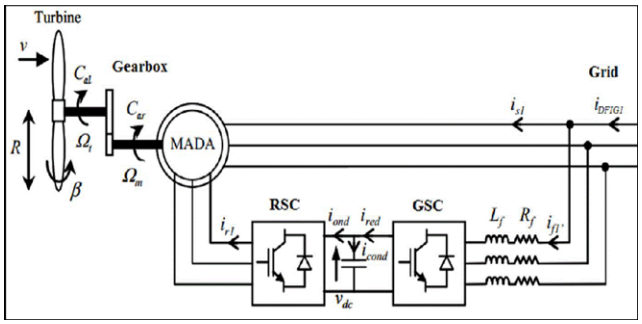

Figure 1: Structure of a wind energy system based on DFIG.

Subsequently, we present a model of DFIG in the landmark Park, and the general principle of the control of two power converters. We conclude by presenting the simulation results and their interpretation.

Modeling of Wind Turbine

By applying the theory of momentum and Bernoulli's theorem, we can determine the incident power (the theoretical power) due to wind [6,7]:

$$P_{incident} = \frac{1}{2}.\rho.S.v^2 \quad (1)$$

S : the surface swept by the blades of the turbine m^2

ρ : the density of air ($\rho = 1,225 kg/m^2$ at atmospheric pressure).

v : wind speed ($T_{sa} = \frac{1}{2\Omega_t} C_p(\lambda,\beta)\rho S v^3$ m/s)

In a wind energy system, due to various losses, the power extracted from provided on the rotor of the turbine is less than the incident power. The power extracted is expressed by [8]:

$$P_{extract} = \frac{1}{2}.\rho.S.C_p(\lambda,\beta).v^3 \quad (2)$$

C_p (λ,β) is called the power coefficient, which expresses the aerodynamic efficiency of the turbine. It depends on the ratio, which is the ratio between the speed at the end of the blades and the wind speed, and the orientation angle β of the blades. The ratio λ can be expressed by the following equation (8,9):

$$\lambda = \frac{\Omega_t.R}{v} \quad (3)$$

Ω: The turbine speed of rotation (rad/s).

R: The length of a blade.

The maximum of power coefficient C_p was determined by Albert

***Corresponding author:** Marouan Elazzaoui, Department of Electrical Engineering, Electronic Power and Control Laboratory, Mohammedia School of Engineering Université Mohammed V-Agdal, Morocco, E-mail: marouan.elazzaoui@gmail.com

Received January 15, 2015; **Accepted** March 03, 2015; **Published** April 04, 2015

Citation: Elazzaoui M (2015) Modeling and Control of a Wind System Based Doubly Fed Induction Generator: Optimization of the Power Produced. J Electr Electron Syst 4: 141. doi:10.4172/2332-0796.10001141

Betz as follows:

$$C_{p\_max}(\lambda,\beta)=\frac{16}{27}=0,5926 \quad (4)$$

The power coefficient is intrinsic to the formation of wind turbine and depends on the profiles of the blades. The power coefficient can be modeled with a single equation that depends on the speed ratio λ and the orientation angle β of the blades as follows:

$$C_{p\_max}(\lambda,\beta)=(0.5-0.0167.(\beta-2))\sin\left[\frac{\pi(\lambda+0.1)}{18.5-0.3(\beta-2)}\right]-0.00184.(\lambda-3)(\beta-2) \quad (5)$$

The Figure 2 shows curves of the power coefficient as a function of λ for various β values. This gives a maximum power coefficient of 0.5 for a speed ratio λ which is 9.13 maintaining β at 2°. By setting β and λ respectively to their optimal values, the wind system will provide optimum electrical power.

The aerodynamic torque on the slow axis is expressed by:

$$T_{sa}=\frac{1}{2\Omega_t}C_p(\lambda,\beta)\rho S v^3 \quad (6)$$

Mechanical speed is related to the speed of rotation of the turbine by the coefficient of the gearbox. The torque on the slow axis is connected to the torque on the fast axis (generator side) by the coefficient of the gearbox (Figure 3).

The total inertia J is made up of the inertia of the turbine plotted on the generator rotor and inertia of the generator:

$$J=\frac{J_t}{G^2}+J_g \quad (7)$$

$$\begin{cases} P_s=-v_{sq}\dfrac{M}{L_s}i_{rq} \\ Q_s=v_{sq}{}^2-\dfrac{M.v_{sq}}{L_s}i_{rd} \end{cases}$$

J_t : inertia of the turbine.

J_g : inertia of the generator.

To determine the evolution of the mechanical speed from total torque T_{mec} applied to the rotor of DFIG, we apply the fundamental equation of dynamics:

$$J=\frac{d\Omega_m}{dt}=T_{mec}=T_{fa}-T_{em}-f\Omega_m \quad (8)$$

Ω: mechanical speed of DFIG.

T_{fa} : aerodynamic torque on the fast axis of the turbine.

T_{em}: Electromagnetic torque.

$f\Omega_m$: coefficient of friction.

The previous equations used to establish the block diagram of the turbine model.

Maximum Power Extraction

In order to capture the maximum power of the incident wind, permanently must adjust the rotational speed of the turbine to the wind. An erroneous speed measurement therefore inevitably leads to degradation of the received power that is why most wind turbines are controlled without control of the speed. The controller in this case should impose a reference torque to allow DFIG turning at an adjustable speed to ensure optimal operating point of power extraction. In this context, the ratio of the speed of wind λ must be maintained at its optimum value $\lambda=\lambda_{opt}$ on a certain wind speed range. Thus, the power coefficient would be maintained at its maximum value (Figure 4).

Modelling of DFIG

The electrical equations of DFIG in the dq reference can be written equation 9,11:

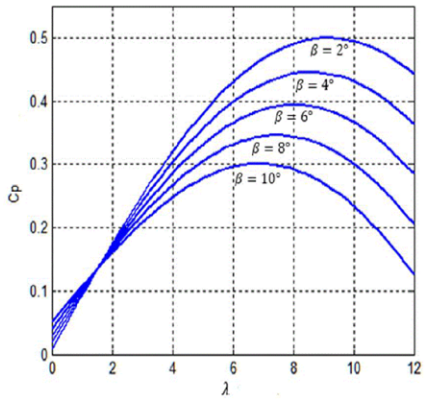

Figure 2: Power coefficient as a function of λ for various β values.

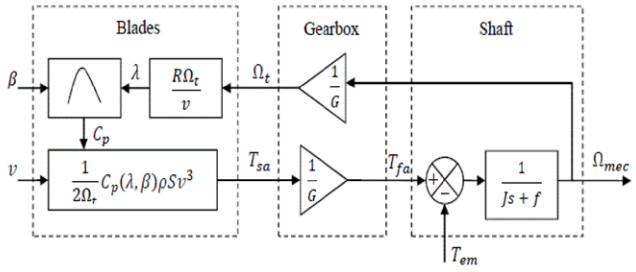

Figure 3: Block diagram of the turbine model.

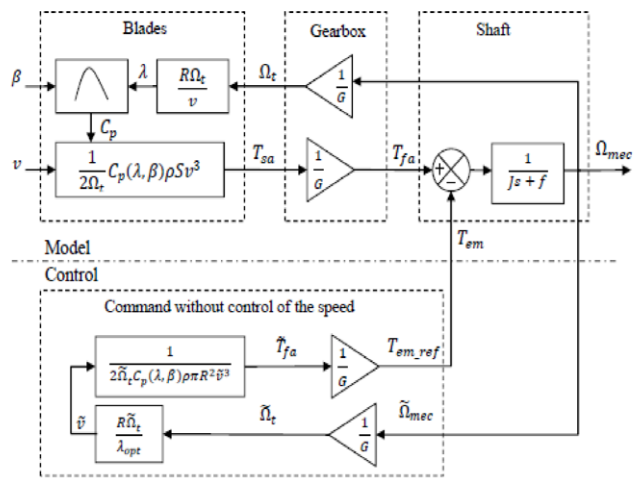

Figure 4: Block diagram without control of the speed.

$$\begin{cases} v_{sd} = R_s i_{sd} + \dfrac{d\varphi_{sd}}{dt} - \omega_s \varphi_{sq} \\ v_{sq} = R_s i_{sq} + \dfrac{d\varphi_{sq}}{dt} - \omega_s \varphi_{sd} \\ v_{rd} = R_r i_{rd} + \dfrac{d\varphi_{rd}}{dt} - \omega_r \varphi_{rq} \\ v_{rq} = R_r i_{rq} + \dfrac{d\varphi_{rq}}{dt} - \omega_r \varphi_{rd} \end{cases} \quad (9)$$

The pulse of the stator currents being constant, the rotor pulse is derived by:

$$\omega_r = \omega_s - p\Omega_m \quad (10)$$

The equations for the flux in dq reference are given by:

$$\begin{cases} \varphi_{sd} = L_s i_{sd} + M i_{rd} \\ \varphi_{sq} = L_s i_{sq} + M i_{rq} \\ \varphi_{rd} = L_r i_{sd} + M i_{sd} \\ \varphi_{rq} = L_r i_{rq} + M i_{sq} \end{cases}$$

With:

$L_s = l_s - M_s, L_r = l_r - M_r$: Cyclic inductances of stator and rotor phase. l_s et l_r inductors own stator and rotor of the machine. M_s et M_r mutual inductances between two stator phases and between two rotor phases of the machine.

M: maximum mutual inductance between stator and rotor stage.

p: number of pairs of poles of the DFIG.

The expression of the electromagnetic torque of the DFIG based on the flow and stator currents is written as follows:

$$T_{em} = p(\varphi_{sd} i_{sd} - \varphi_{sq} i_{sd}) \quad (12)$$

The active and reactive power of the stator and rotor are written as follows (9,11):

$$\begin{cases} P_s = v_{sd} i_{sd} + v_{sq} i_{sq} \\ Q_s = v_{sq} i_{sd} + v_{sd} i_{sq} \\ P_r = v_{rd} i_{rd} + v_{sq} i_{rq} \\ Q_s = v_{rq} i_{rd} + v_{rd} i_{rq} \end{cases} \quad (13)$$

Vector Control of DFIG

DFIG control strategies are based on two different approaches (12):

- Flow control in closed loop, where the frequency and voltage are considered variables (unstable grid).
- Flow control in open loop when the voltage and frequency are constant (stable grid).

In our study, the frequency and voltage are assumed to be constant. We can see from equation (12), the strong coupling between flows and currents. Indeed, the electromagnetic torque is the cross product between flows and stator currents, making the control of DFIG particularly difficult. To simplify ordering, we approximate the model to that of the DC machine which has the advantage of having a natural coupling between flows and currents. For this, we apply vector control, also known order by direction of flow. We choose dq reference linked to the rotating field (Figure 5).

Stator flux φ_s is oriented along the axis. Thus, we can write:

$$\begin{cases} \varphi_{sd} = \varphi_s \\ \varphi_{sq} = 0 \end{cases} \quad (14)$$

$$\begin{cases} \varphi_{sd} = L_s i_{sd} + M i_{rd} = \varphi_s \\ \varphi_{sq} = L_s i_{sq} + M i_{rq} = 0 \end{cases} \quad (15)$$

In the field of production of wind energy, these are average machines and high power which are mainly used. Thus, we neglect the stator resistance. Taking the constant stator flux we can write:

$$\begin{cases} v_{sd} = 0 \\ v_{sq} = V_s = \omega_s \varphi_s \end{cases} \quad (16)$$

To determine the angles necessary for transformation Park of the stator variables θ_s and the rotor variables θ_r, we used a phase locked loop (PLL) as shown in Figure 6. This PLL allows to accurately estimate the frequency and amplitude of the grid (13). The architecture of the controller is shown in Figure 7. It is based on the three-phase model of the electromechanical conversion chain of the wind energy system. From Figure 7, three commands are needed:

- The maximum extraction control wind power by controlling said MPPT (detailed in Section III).
- Control of RSC by controlling the electromagnetic torque and stator reactive power of DFIG.
- Control of GSC by controlling the voltage of the DC bus and the active and reactive power exchanged with the grid.

Control of the rotor side converter (RSC)

The principle of the Control of the rotor side converter is shown in Figure 8. The Controls of electromagnetic torque and stator reactive power will be obtained by controlling the rotor dq axes currents of DFIG. From the equations (15) and (16) we obtain the expression of the stator current:

$$\begin{cases} i_{sd} = \dfrac{v_{sq}}{\omega_s L_s} - \dfrac{M}{L_s} i_{rd} \\ i_{sq} = -\dfrac{M}{L_S} i_{rq} \end{cases} \quad (17)$$

These expressions are then substituted in the equation (11) of the rotor flux which then become:

$$\begin{cases} \varphi_{rd} = \sigma L_r i_{rd} + \dfrac{M v_{sq}}{\omega_s L_s} \\ \varphi_{rq} = \sigma L_r i_{rq} \end{cases} \quad (18)$$

With:

$\sigma = 1 - \dfrac{M^2}{L_r L_s}$: the dispersion coefficient of the DFIG Substituting the expressions of the direct and quadrature components of the rotor flux in the equation (9) we get:

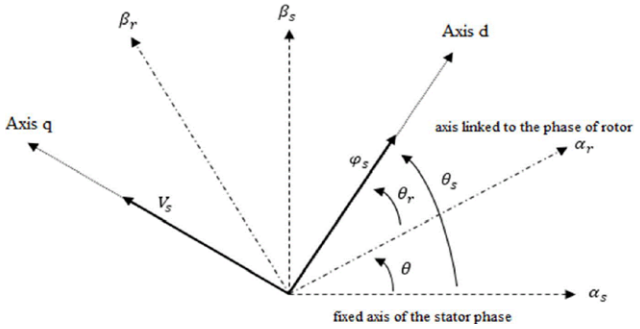

Figure 5: Orientation of the axis d to stator flux.

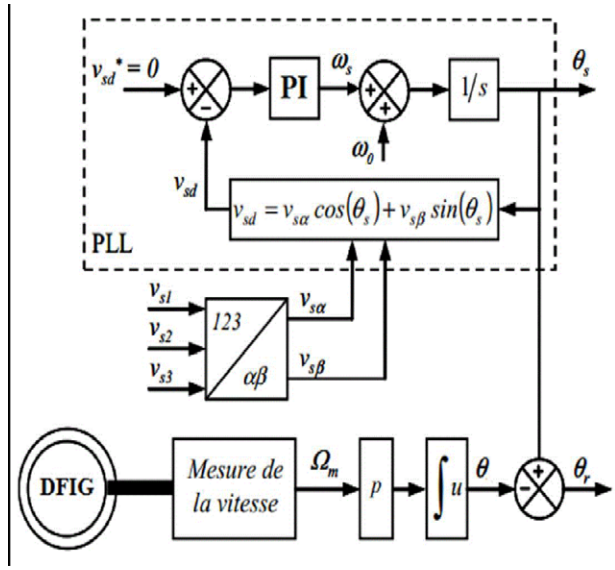

Figure 6: Establishment angles processing using a PLL.

$$\begin{cases} v_{rd} = R_r i_{rd} + \sigma L_r \frac{di_{rd}}{dt} + e_{rd} \\ v_{rq} = R_r i_{rq} + \sigma L_r \frac{di_{rd}}{dt} + e_{rq} + e_{\phi} \end{cases}$$

With:

$$e_{rd} = -\sigma L_r \omega_r i_{rq}; e_{rq} = \sigma L_r \omega_r i_{rd}; e_{\phi} = \frac{\omega_r M V_{sq}}{\omega_s L_s}$$

The expression of the electromagnetic torque becomes:

$$T_{em} = -\frac{pMv_{sq}}{\omega_s L_s} i_{rq} \quad (20)$$

Stator active and reactive powers are expressed by:

$$\begin{cases} P_s = -v_{sq} \frac{M}{L_s} i_{rq} \\ Q_s = v_{sq}^2 - \frac{M.v_{sq}}{L_s} i_{rd} \end{cases} \quad (21)$$

These last expressions show that the choice of coordinate system (dq) makes the electromagnetic torque produced by the DFIG, and therefore the stator power, proportional to the current of the rotor axis (q). The stator reactive power, in turn, is proportional to the current of the rotor axis (d) due to a constant imposed by the grid. Thus, these stator powers can be controlled independently of one another. This shows us that we can set up a control rotor currents due to the influence of the couplings, every current can be controlled independently each with its own controller. The reference values for these regulators will be the rotor axis current (q) and the rotor axis current (d). The block diagram of the control loops of the axis rotor currents (dq) is shown in Figure 9, the regulators used are PI correctors.

The rotor current of the reference axis (q) is derived from the MPPT control via the electromagnetic torque reference (Figure 4). The rotor current of the reference axis (d) is, in turn, derived from the control of the stator reactive power.

From the equations (20) and (21) we obtain:

$$i_{rd}^{*} = -\frac{L_s}{M.v_{sq}} Q_s^{*} + \frac{v_{sq}}{\omega_s M} \quad (22)$$

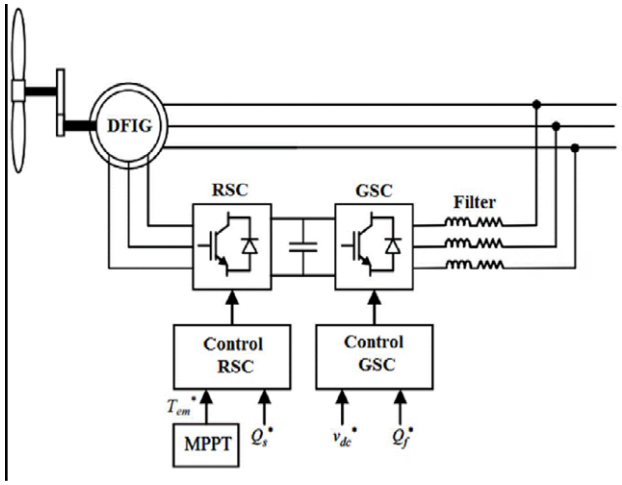

Figure 7: Control architecture of the wind system.

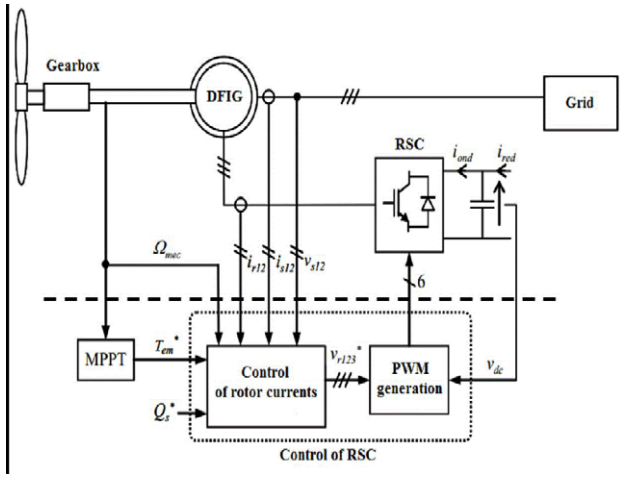

Figure 8: Principle of the Control of the rotor side converter (RSC).

$$i_{rd}^{*} = -\frac{\omega_s L_s}{pMv_{sq}} T_{em}^{*} \quad (23)$$

Figure 10 shows the block diagram of the control of RSC. Figure 11 show the principle of the Control of the rotor side converter performs the following two functions:

- Control currents flowing in the RL filter.
- Control voltage of the DC bus.

Control currents flowing in the RL filter

According to Kirchhoff's laws, the equations of the filter in the three-phase reference voltages are given by:

$$\begin{cases} V_{f1} = -R_f i_{f1} - L_f \frac{di_{f1}}{dt} + V_{s1} \\ v_{f2} = -R_f i_{f2} - L_f \frac{di_{f2}}{dt} + V_{s2} \\ V_{fa} = -R_f i_{fa} - L_f \frac{di_{fa}}{dt} + V_{sa} \end{cases} \quad (24)$$

Applying the Park transformation, we obtain: P_f^{*}

$$\begin{cases} v_{fd} = -R_f i_{fd} - L_f \frac{di_{fd}}{dt} + e_{fd} \\ v_{fq} = -R_f i_{fq} - L_f \frac{di_{fq}}{dt} - \omega L_f i_{fq} + e_{fq} \end{cases} \quad (25)$$

With:

$$e_{fd} = \omega_s L_f i_{fd}; e_{fq} = -\omega_s L_f i_{fd} + v_{sq}$$

The pattern of binding of GSC to grid in the landmark Park along the stator rotating field shows us that we can put in place a control of the currents flowing in the RL filter is given to the influence of the couplings, every axis can be controlled independently with each its own PI controller. The reference values for these controllers will be current in RL filter axes (dq) (Figure 12). The reference currents i_{fd}^{*} and i_{fq}^{*} are respectively the voltage from the control block of the DC bus and control of reactive power at the GSC connection point to the grid (Figure 11).

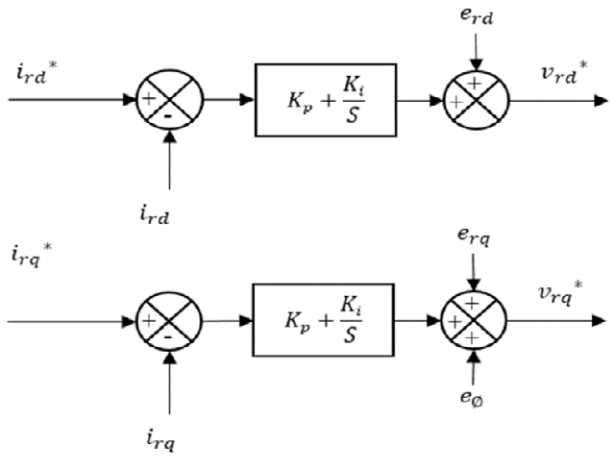

Figure 9: Control of rotor currents.

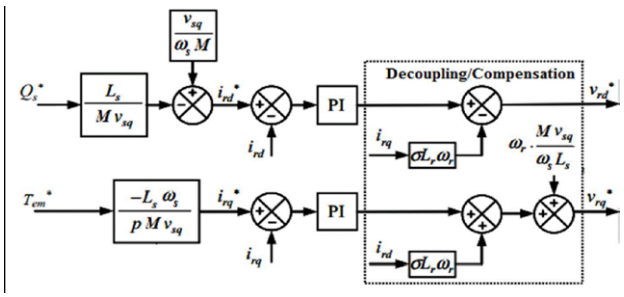

Figure 10: Control of RSC.

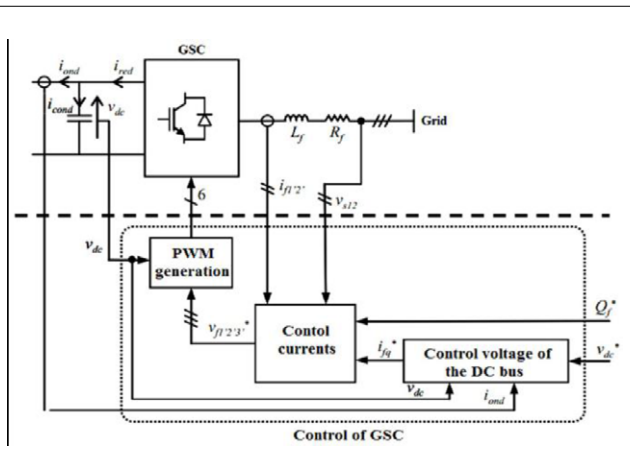

Figure 11: Principle of the Control of the grid side converter (GSC).

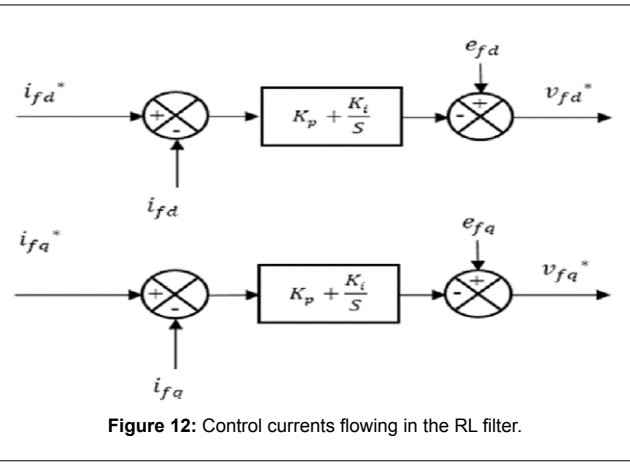

Figure 12: Control currents flowing in the RL filter.

Neglecting losses in the resistance of RL filter and taking the orientation of the coordinate system (dq) connected to the rotary stator field v_{sd}=0 the equations for the powers generated by the GSC are given by:

$$\begin{cases} P_f = v_{sq} i_{fq} \\ Q_f = v_{sq} i_{fd} \end{cases} \quad (26)$$

From these equations, it is possible to impose the active and reactive power reference noted here P_f^{*} and Q_f^{*} imposing the following reference currents:

$$\begin{cases} i_{fd}^{*} = \dfrac{Q_f^{*}}{v_{sq}} \\ i_{fq}^{*} = \dfrac{P_f^{*}}{v_{sq}} \end{cases} \quad (27)$$

Control of the DC bus voltage

We can express the powers involved on the DC bus by:

$$\begin{cases} P_{red} = v_{dc} i_{red} \\ P_c = v_{dc} i_{cond} \\ P_{ond} = v_{dc} i_{ond} \end{cases} \quad (28)$$

These powers are linked by the relation:

$$P_{red} = P_c + P_{ond} \quad (29)$$

Neglecting all the Joule losses (losses in the capacitor, the converter and the RL filter), we can write:

$$P_f = P_{red} = P_c + P_{ond} \quad (30)$$

By adjusting the power P_f, then it is possible to control the power P_c in the capacitor and therefore to regulate the DC bus voltage. To do this, the P_{ond} and powers must be known to determine P_f^{*}. The reference power for the capacitor is connected to the reference current flowing through the capacitor:

$$P_c^{*} = v_{dc} i_{cond}^{*} \quad (31)$$

Regulating the DC bus voltage is then effected by an external loop (with respect to the inner loop control of current), for maintaining a constant voltage on the DC bus, with a PI controller that generates the reference current i_c^{*} in the capacitor (Figure 13). Figure 14 shows the block diagram of the control of GSC. This block diagram includes the terms of decoupling and compensation to be able to independently control the (dq) axes currents circulating in the RL filter and the active and reactive power exchanged between the GSC and the grid.

Simulation Results

The simulations of the whole system were performed with Matlab/Simulink, the DC bus reference voltage, denoted V_{dc}^{*} is set at 1200 V. The reactive power references Q_s^{*} and Q_f^{*} are set to 0 VAr, ensuring unity power factor. We present in this section the results of the proposed control. Figure 15 illustrates the profile of the average wind speed used for simulation, while Figure 16 shows the shaft rotational speed derived by the turbine. The figures (Figures 17 and 18) show that the electromagnetic torque and reactive power provided by DFIG follow their references, this is due to control of direct and quadrature components of the rotor current. Figure 19 illustrates the power stator

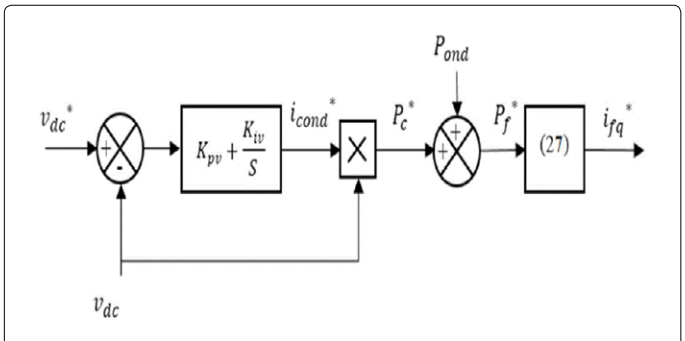

Figure 13: Control loop of the DC bus voltage.

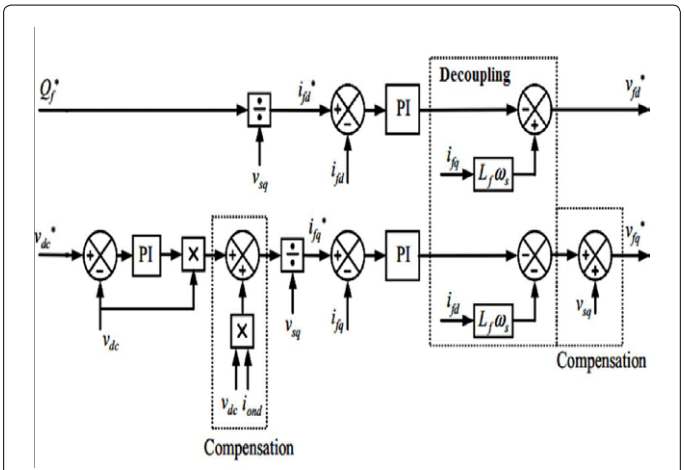

Figure 14: Control of GSC.

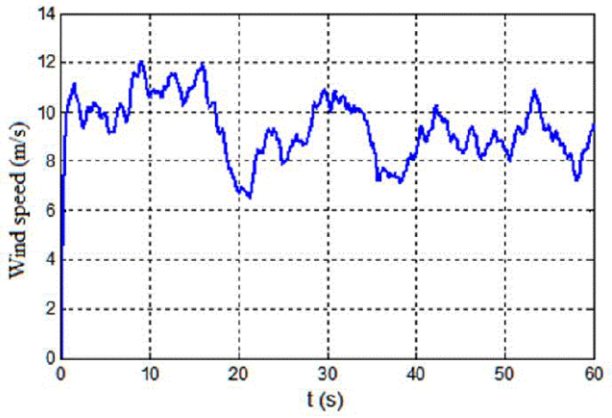

Figure 15: Wind speed.

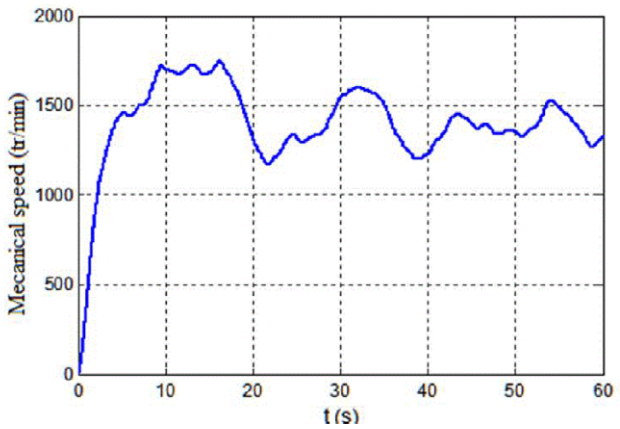

Figure 16: Mechanical speed.

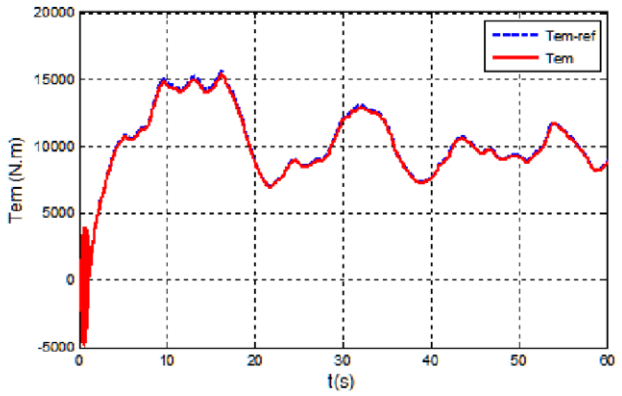

Figure 17: Electromagnetic torque (reference and simulated).

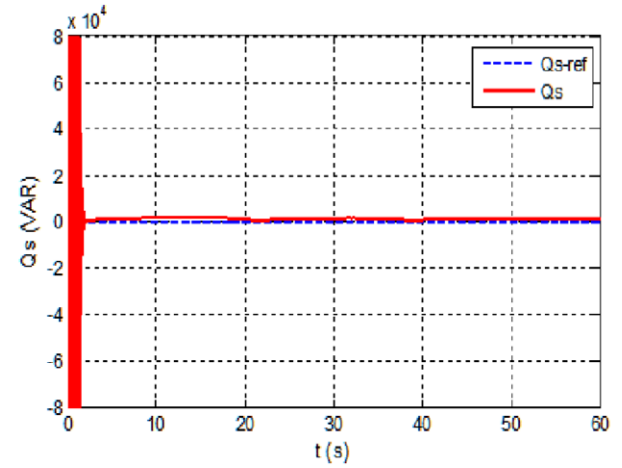

Figure 18: Stator reactive power (reference and simulated).

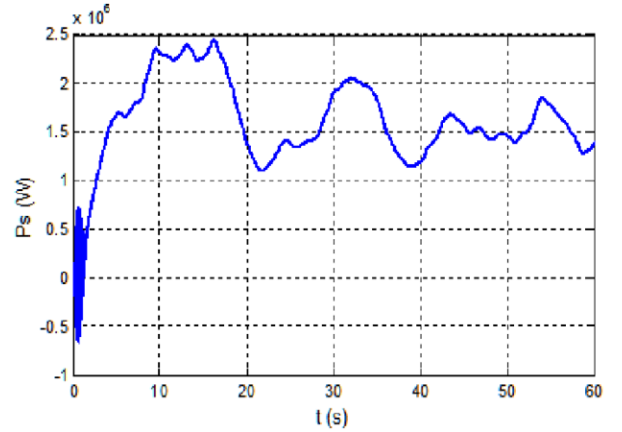

Figure 19: Stator active power.

extracted, and Figure 20 shows that the DC bus voltage is perfectly regulated. We see in Figure 21 that the current delivered by the wind system is in phase with respect to the supply voltage, this confirms that the wind system injects the active power into the grid.

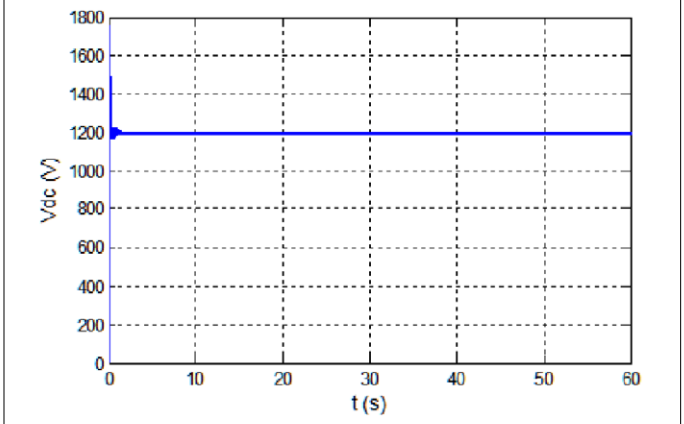

Figure 20: DC bus voltage.

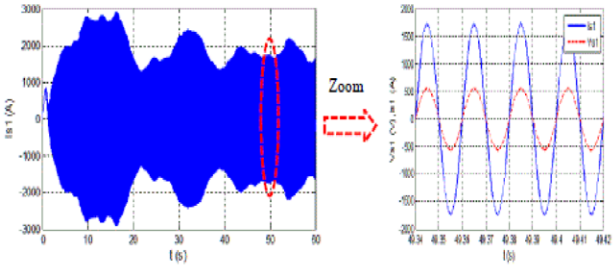

Figure 21: Stator current evolution.

Conclusion

This paper is devoted to modeling, simulation and analysis of a wind turbine operating at variable speed. Stable operation of the wind energy system was obtained with the application of the control direction of the flow. The overall operation of the wind turbine and its control system were illustrated in transient and permanent regimes. DFIG operates in two quadrants. Operation hyposynchronous for positive slip and hypersynchronous operation for a negative slippage. The generator supplied power to the grid with an active power regardless of the mode of operation. The control strategy based on the PI control with correction was tested. Simulation results show that the proposed wind energy system is feasible and has many benefits.

References

1. Ackermann T (2002), An Overview of Wind Energy-Status 2002, Renewable and Sustainable Energy Reviews 6: 67-127.
2. http://www.gepower.com/prod_serv/products/wind_trubines/en/index.html
3. Burton T, Sharpe D, Jenkins N (2001) Wind Energy Handbook, John Wiley&Sons, Ltd.
4. Kling WL, Slootweg JG (2002) Wind Turbines as Power Plants, Oslo, Norway: in Proceeding of the IEEE/Cigré workshop on Wind Power and the impacts on Power Systems.
5. Xu L, Wei C (1995) Torque and Reactive Power Control of a Doubly Fed Induction Machine by Position Sensorless Scheme. IEEE Trans, Industry Application.
6. Alesina A, Venturini M (1988) Intrinsic Amplitude Limits and Optimum Design of 9 Switches Direct PWM AC-AC converter, Proc. of PESC, 1284-1290.

7. Seyoum D, Grantham C (2003) Terminal Voltage Control of a Wind Turbine Driven Isolated Induction Generator using Stator Oriented Field Control, IEEE Transactions on Industry Applications, 846-852.

8. Davigany A (2007) «Participation aux services système de fermes éoliennes à vitesse variable integrant un stockage inertiel d'énergie,» Thèse de Doctorat, USTL Lille.